Djungar Gate Kazakhstan

Estimate of Wind Speed
Energy Yield Prediction

12.9.2005

Client:
UNDP Kazakhstan
67 Tole bi street
Almaty, 480091
Kazakhstan

Wind Solutions
Engelsgrube 25
23552 Lübeck
Germany

Index

List of Tables

List of Figures

Disclaimer

Wind Solutions has not conducted measurements at the sites. Hence Wind Solutions accepts no responsibility for the accuracy of the data supplied to it. Furthermore Wind Solutions cannot be held responsible for incomplete information.

1 Introduction

A pilot project is to be developed at Djungar Gate In Kazakhstan. Wind Solutions has been instructed by UNDP Kazakhstan to carry out an independent assessment of the wind climate of the proposed wind farm and estimate the energy yield. Furthermore two layouts are to be developed for the pilot project for two different sizes of wind turbines. These layouts have been analysed here, in conjunction with the results of the wind analysis, to predict the energy yield. The results of the work are reported here.

A description of the long-term wind climate at a potential wind farm is best determined using wind data recorded at the site. UNDP Kazakhstan has supplied data recorded at the site.

It is noted that Wind Solutions has not conducted wind measurements itself at the site and cannot, therefore, be responsible for the accuracy of the data supplied to it.

Following steps have been undertaken for this analysis:

1. Developing a 3-dimensional topographic map
2. Estimating the surface roughness (on the basis of photos)
3. Quality control and plausibility check of provided data
    - Review of calibration
    - Checking quality (mounting, calibration, position etc. on basis of site visit)
    - Checking for gaps and faulty values
4. Correlation of the data with suitable long-term meteorological station
5. Performing flow modelling (WAsP) on the basis of the resulting estimated wind climate, 3-dimensional map and estimated surface roughness
6. Estimating turbulence and extreme wind speeds on the basis of the provided data to classify the site
7. Choice of suitable wind turbine together with client on the basis of the site classification
8. Prediction of on-site air density
9. Micro-Siting (2 different options for 2 different ranges of wind turbine sizes)
10. Estimating energy yield for the selected turbine types including wake modelling to establish array losses
11. Uncertainty analysis (exceedance probability)

2 Description of the Site

2.1 General

The project Djungar Gate is situated in the east of Kazakhstan close to the Chinese border. The site is approximately 35 km south-east of lake Alakul. Towards west in less than 10km is the settlement Tokty.

A map of the site location and surrounding area is shown in Figure 1.

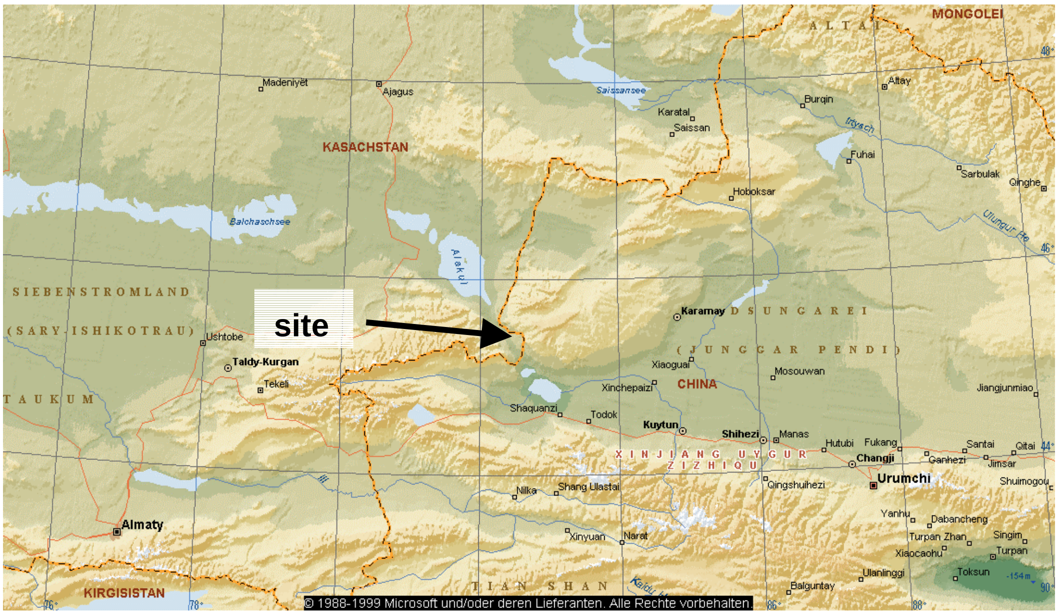

Figure 1: Djungar Gate

The area has a very special topography. The site is located in a narrow gap of less than 15km width between two large mountainous areas which form a wind tunnel. While the elevation of the gap is as low as 380 to 500m the mountains reach quickly a height of 1600m and more.

The planned project consists of 5 MW installed capacity. According to the client the size of the planned turbines is approximately 850kW to 2 MW, hence the rotor diameters range from approximately 50 to 80m.

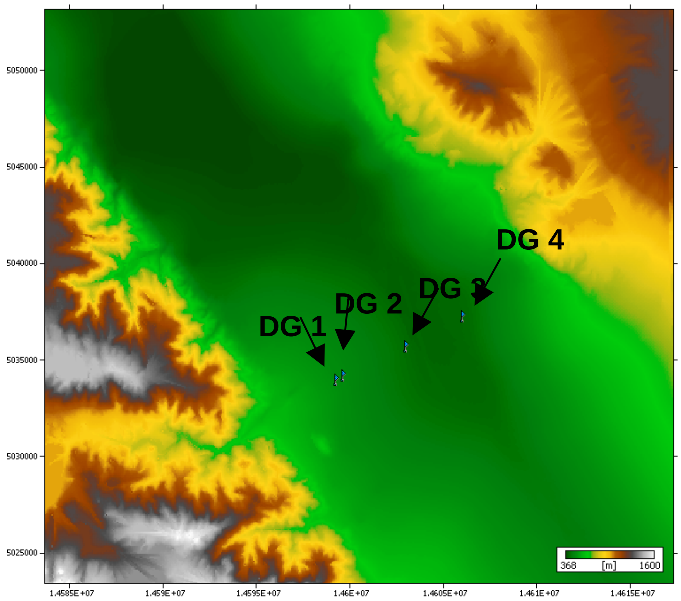

Figure 2: Elevation indicating position of masts

Please note that the provided topographic map which is the basis for the 3-dirmensional height model has a scale of only 1:100000. Contour lines are only displayed every 40m, in flatter parts of the terrain every 20m. Generally a minimum distance of 10m between the height contour lines is recommended.

2.2 Roughness

Topographic maps of the scale 1:100,000 have been provided together with some photos have been provided to document the surface roughness (Figure 3).

Figure 3: Djungar Gate D2 looking NE

Additionally information has been obtained from Google Earth.

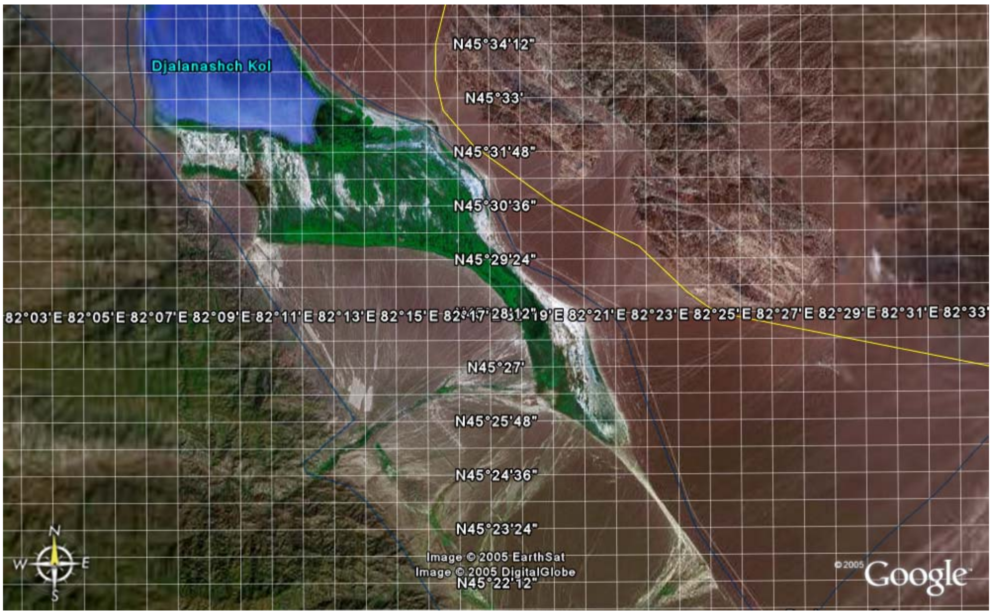

Figure 4: Satellite picture Djungar Gate

The majority of the site is made up of bare ground with short grass interrupted by patches of higher vegetation mainly along discharges of the adjacent mountains. Towards north the lake Zhalanoshkol dominates the valley.

In general the appearance of the landscape is very open.

Following the Davenport classification and the recommendations in /1/ a surface roughness length of 0.05 m has been assigned to the grassy areas, which corresponds to roughness class 1.4. A roughness length of 0.06 m corresponding to roughness class 1.6 was found to be appropriate for the slopes of the mountains. The discharge south of the lake Zhalanoshkol has been described by a roughness length of 0.06 m corresponding to roughness class 1.6. The lake itself has a roughness length of 0m.

Following map indicates the surface roughness lengths.

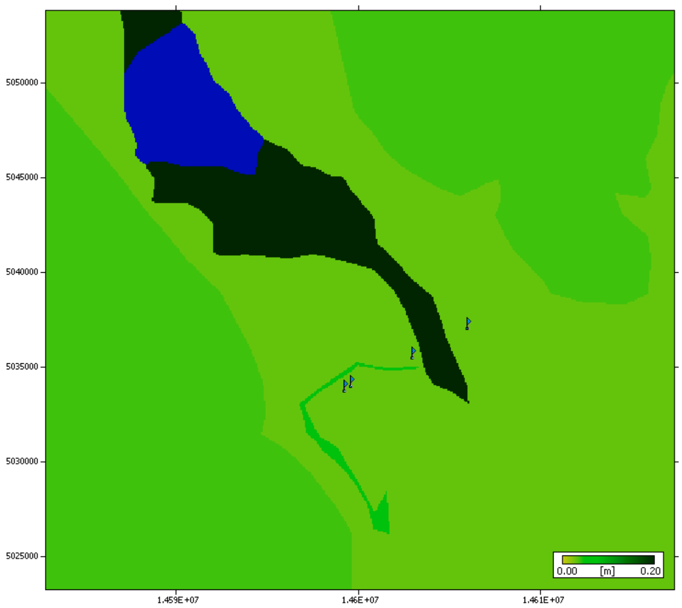

Figure 5: Roughness map indicating roughness length

3 Description of the Monitoring Equipment

3.1 General

Measurements are conducted on the site. Data from the measurement masts and details of the monitoring equipment used at the site have been supplied by the client to Wind Solutions. Please note that Wind Solutions has not visited the site.

The mast is located at following co-ordinates:

Station	Latitude	Longitude	Grid E	Grid N
DG1	45°25.88'	82°16.09'	14599239	5033752
DG2	45°26.01'	82°16.39'	14599627	5033999
DG3	45°26.79'	82°18.99'	14602994	5035499
DG4	45°27.61'	82°21.34'	14606033	5037069

Table 1: Position of measurement masts /7/

The measurement masts are positioned across the width of the valley. The future wind farm shall be located in the vicinity of the measurement masts.

Measurement started in April 1998. Data has been provided until April 2000.

Station	Start	End	Comments
DG1	8.4.98	19.7.99	-
DG2	10.4.98	16.4.00	Anemometer at 26.4 (Vaisala) failed most of the time, larger data gaps from 6. – 25.1.99, 8. – 28.3.99, 9. – 31.10.99 and 5.12.99 – 9.1.00 due to vane failure
DG3	10.4.98	22.5.00	-
DG4	10.4.98	22.5.00	Anemometer at 26.4 (Vaisala) failed most of the time, larger data gaps from 4. – 25.1.99, 8. – 28.3.99, 21. – 31.10.99 and 5.12.99 – 9.1.00 due to vane failure

Table 2: Measurement Periods

3.2 Mounting

The masts comprise of triangle lattice mast.

Figure 6: Side booms /7/

The length of the side booms is about 2.5 meter of which approximately 0.5 meter are used to fix the side booms to the mast. The orientation of the booms is to the south-west /2/. The instruments are thus mounted on side booms of the equivalent length of 4 times the lattice mast diameters.

The orientation of the side booms do comprise with the IEA recommendations for wind speed measurements as they are oriented perpendicular to the main wind direction.

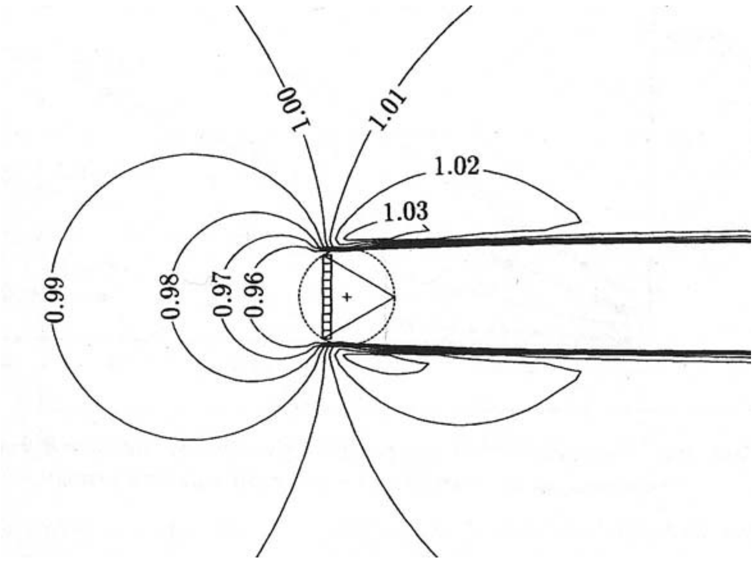

Figure 7: Acceleration around lattice mast /3/

Following table summarises the measurement heights and instrumentation of each mast.

Station	Ws 1 [m]	Sd1 [m]	Gust/lull [m]	Ws 2 [m]	Wd 1 [m]	Wd2 [m]	Temp diff [m]	Others [m]
DG1	10.8	10.8	10.8	-	10.8	-	10.8 – 4.7	-
DG2	26.6	26.6	26.6	10.8	25.4	10.8	25.4 – 4.7	Pressure, ws 3 26.4
DG3	33.0	33.0	33.0	10.7	32.4		32.4 – 4.7	-
DG4	33.1	33.1	33.1	10.6	32.4	-	32.4 – 4.7	-

Table 3: Instrumentation masts /7/

The mast's heights are hence less than the generally recommended 60% of the future turbine height assuming that the future wind turbines do not exceed a hub height of 80m.

3.3 Instrumentation

The datalogger used at the four stations is the Aanderaa Sensor Scanning Unit 3010. The sampling interval used is 10 minutes and a built-in quartz clock triggers scanning.

Wind speed is measured with Risø P2546a Cup Anemometers of the Risø-70 type. The calibration is linear with an offset (`starting speed'). The distance constant is about 1.7 m. The cup anemometers are individually calibrated in wind tunnel.

Wind direction is measured with an Aanderaa Wind Direction Sensor 3590. Inside the housing an electronic compass, comprising four Hall elements, is magnetically coupled to the vane. The inaccuracy is specified to be better than 5 degrees, the threshold speed is less than 0.3 m/s and the operating temperature range is from –40 °C to 50 °C. On the boom the wind vane is orientated towards magnetic north giving true magnetic readings.

Barometric air pressure is measured with an Aanderaa Air Pressure Sensor 2810. The sensor has a measuring range of 920…1080 hPa, a resolution of 0.2 hPa and an inaccuracy specified to ±0.2 hPa. The operating temperature range is from –40 °C to 47 °C.

Air temperature is measured with the Risø P2742a Pt 500-resistance temperature sensor mounted in a Risø P2029a Radiation Shield. The sensor has a measuring range from nominally –44 °C to 49 °C, a resolution of 0.1 °C and a time constant of about one-minute.

The logger has been programmed to record the 10-minute average wind speeds and direction together with the standard deviations of wind speed. Furthermore the maximum and minimum wind speeds as well as the standard deviation of the wind direction are logged.

3.4 Calibration

All anemometers have been calibrated individually before starting the measurements. The result of the calibration has been implemented in the logger so the provided data include the required corrections /7/.

No information has been provided about maintenance of the instruments and re-calibration after each year of operation.

4 Data Analysis

4.1 Wind Speed

The wind data have been subject to a quality checking procedure by Wind Solutions to identify records which were affected by equipment malfunction and other anomalies. Where appropriate, these data have been removed. The basic statistics and data coverage are summarised in following table (incl. the calibration):

	DG1		DG 2				DG 3				DG 4			
	10.8m		26.6m		10.8m		33m		10.7m		33.1m		10.6m	
	average	recovery	average	recovery	average	recovery	average	recovery	average	recovery	average	recovery	average	recovery
Apr-98	8	100% beginning 8.4.98	9	100% beginning 10.4.98	7.7	100% beginning 10.4.98	8.8	100% beginning 10.4.98	7.4	100% beginning 10.4.98	9	100% beginning 10.4.98	7.6	100% beginning 10.4.98
May-98	7.2	100%	8.1	100%	7.2	100%	8.1	100%	6.8	100%	8	100%	6.8	100%
Jun-98	6.2	100%	7	100%	6.3	99%	7.2	100%	6	100%	6.8	100%	5.7	100%
Jul-98	5.5	100%	6.4	99%	5.5	99%	6	100%	5.1	100%	5.8	100%	4.9	100%
Aug-98	5.7	100%	6.6	100%	5.8	100%	6.4	100%	5.3	100%	6.1	100%	5.1	100%
Sep-98	7.1	100%	8.1	100%	7.2	100%	7.9	100%	6.5	100%	7.9	100%	6.4	100%
Oct-98	7.8	100%	9	100%	8	100%	8.9	100%	7.3	100%	9.1	100%	7.5	100%
Nov-98	8	100%	9.1	100%	8.1	100%	8.9	100%	7.4	100%	8.9	100%	7.4	100%
Dec-98	8.5	100%	9.3	100%	8.7	100%	9.9	100%	8.5	100%	10.5	100%	9.2	100%
Jan-99	9.3	100%	9.2	37%	8.4	37%	9.9	100%	8.6	100%	8.4	100%	7.1	100%
Feb-99	10.3	100%	11.7	100%	10.5	100%	11.6	100%	9.7	100%	12	100%	10.1	100%
Mar-99	8.5	100%	8.7	35%	8	35%	9.3	100%	7.8	100%	8.4	100%	7.2	100%
Apr-99	6.6	100%	7.7	100%	6.7	100%	7.6	100%	6.3	100%	7.4	100%	6.2	100%
May-99	6.9	100%	7.8	100%	7	100%	7.8	100%	6.5	100%	7.7	100%	6.5	100%
Jun-99	6.1	100%	7.1	100%	6.2	100%	6.8	100%	5.7	100%	6.6	100%	5.5	100%
Jul-99	5.8	100% ending 19.7.99	6.7	99%	5.9	99%	6.7	100%	5.5	100%	6.2	100%	5.1	100%
Aug-99			8.1	92%	7.1	92%	7.6	100%	6.3	100%	7.7	100%	6.4	100%
Sep-99			7.9	100%	6.9	100%	7.7	100%	6.3	100%	7.8	100%	6.4	100%
Oct-99			5.8	31%	5.1	31%	7.5	100%	6.1	100%	7.5	100%	6.1	100%
Nov-99			11.1	100%	9.8	100%	10.7	100%	9	100%	11.3	100%	9.5	100%
Dec-99			12.6	14%	11.3	14%	10.4	100%	8.8	100%	12.6	100%	10.7	100%
Jan-00			11.2	73%	10.1	73%	11.6	100%	9.8	100%	12.8	100%	10.8	100%
Feb-00			10.7	100%	9.6	100%	10.8	100%	9.1	100%	11.1	100%	9.4	100%
Mar-00			9.6	100%	8.5	100%	9.6	100%	8.1	100%	9.9	100%	8.3	100%
Apr-00			8.7	100% ending 16.4.00	7.7	100% ending 16.4.00	7.9	100%	6.5	100%	7.6	100%	6.4	100%
May-00							7.8	100% ending 22.5.00	6.5	100% ending 22.5.00	7.8	100% ending 22.5.00	6.6	100% ending 22.5.00

Table 4: Basic Statistics

Following table summarises the wind speeds and Weibull parameters for the complete measurement period. The analysis includes the calibration factors. More detailed results can be found in the Appendix.

	Height [m]	A-parameter	Mean Wind Speed [m/s]	k-parameter
DG 1	10.8	8.4	7.4	1.97
DG 2	26.6	9.8	8.6	2.10
	10.8	8.7	7.7	2.00
DG 3	33	9.8	8.7	2.16
	10.7	8.3	7.3	2.05
DG 4	33.1	9.8	8.7	1.98
	10.6	8.2	7.3	1.88

Table 5: Measured wind speeds and Weibull parameters

The measured wind shear exponent α refers to the measured shear between top height and bottom height. The measured wind shear exponent α ranges from 0.131 to 0.153 corresponds in flat terrain under neutral conditions to a roughness length of 0.01m to 0.026m, which is corresponds to the assumptions made (Chapter 2.2).

4.2 Direction

In order to optimise the park layout with respect to the park efficiency the knowledge of the wind direction is crucial. The wind direction can be described in three different ways: frequency, mean wind speed and as the result of the two the energy contents in the wind.

The following figures show mean wind speed, frequency, and the resulting energy roses at the positions of the masts at top height. Since all roses are very similar only DG 2, 3 and 4 are shown as their data sets are the longest and the measurements are the highest above ground.

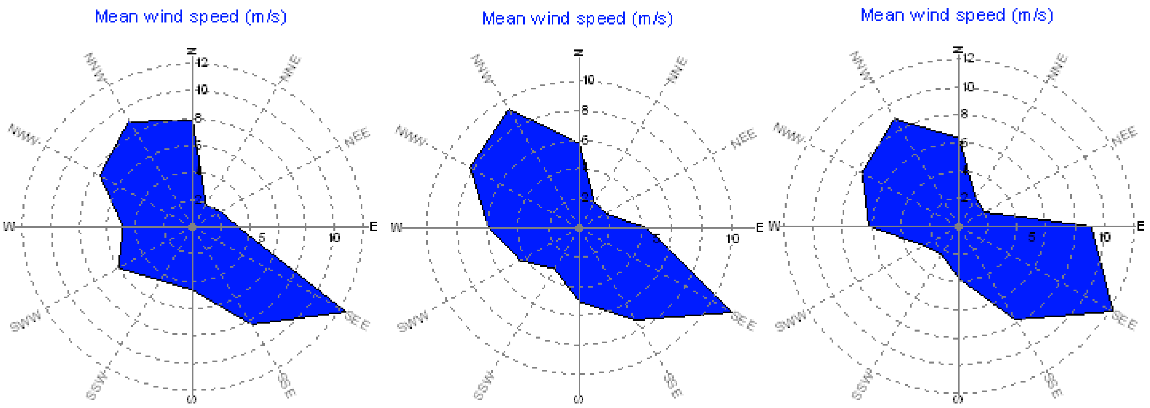

Figure 8: Mean wind speed roses (left DG2, middle DG3, right DG4)

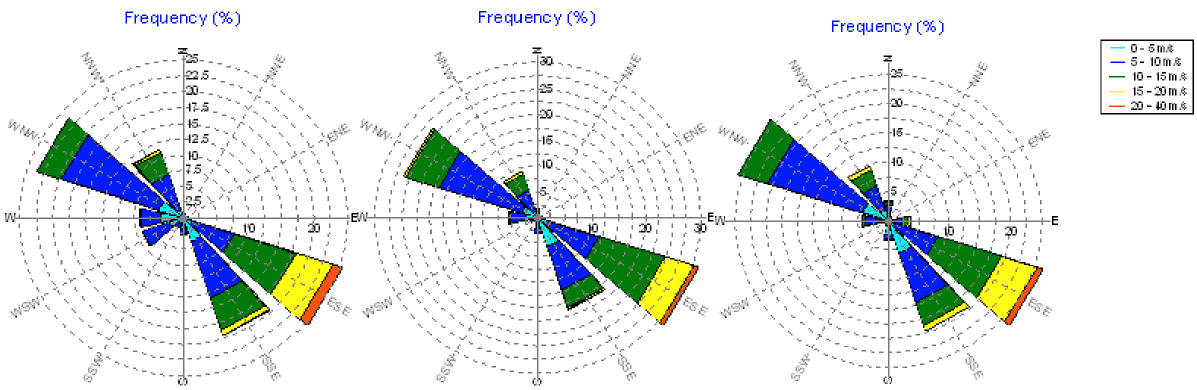

Figure 9: Frequency roses (left DG2, middle DG3, right DG4)

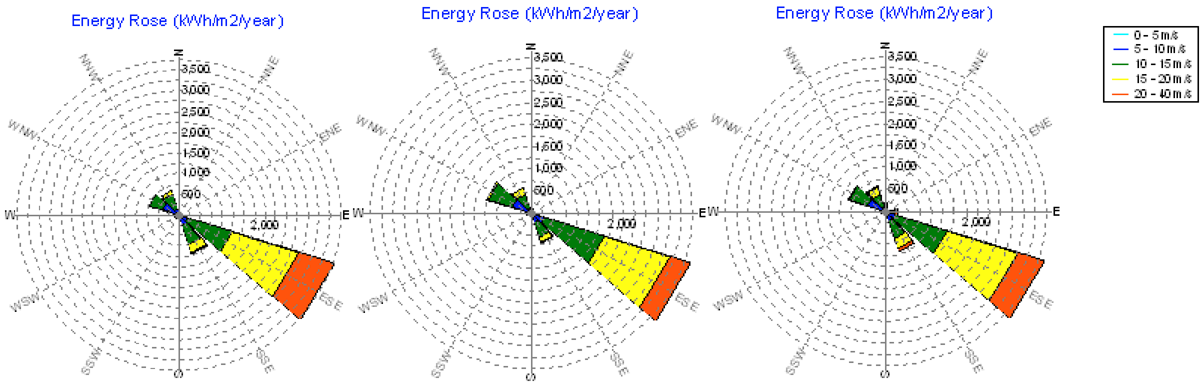

Figure 10: Energy roses (left DG2, middle DG3, right DG4)

The wind direction at Djungar Gates is clearly dominated by two wind directions: WNW and ESE. The mean wind speed per sector as well as the frequency of the ESE sector is bigger than the WSW sector. Thus the energy rose is clearly dominated by the ESE sector.

The wind from WNW occurs mainly during summer and is refered to as “Abin”. “Saikan” is the predominant wind during winter as comes from ESE with much stronger wind speeds than Abin.

Following figures show clearly the change in wind speed during a change of wind direction: Just before the wind turns by 180° the wind speed slows down to very low values. When the wind direction has changes the speed picks up again. This phenomenon can be observed also in the opposite direction.

Please note that the wind direction turns very rapidly in less than 15 minutes. Care has to be taken so that the wind turbine control system adjusts quickly enough.

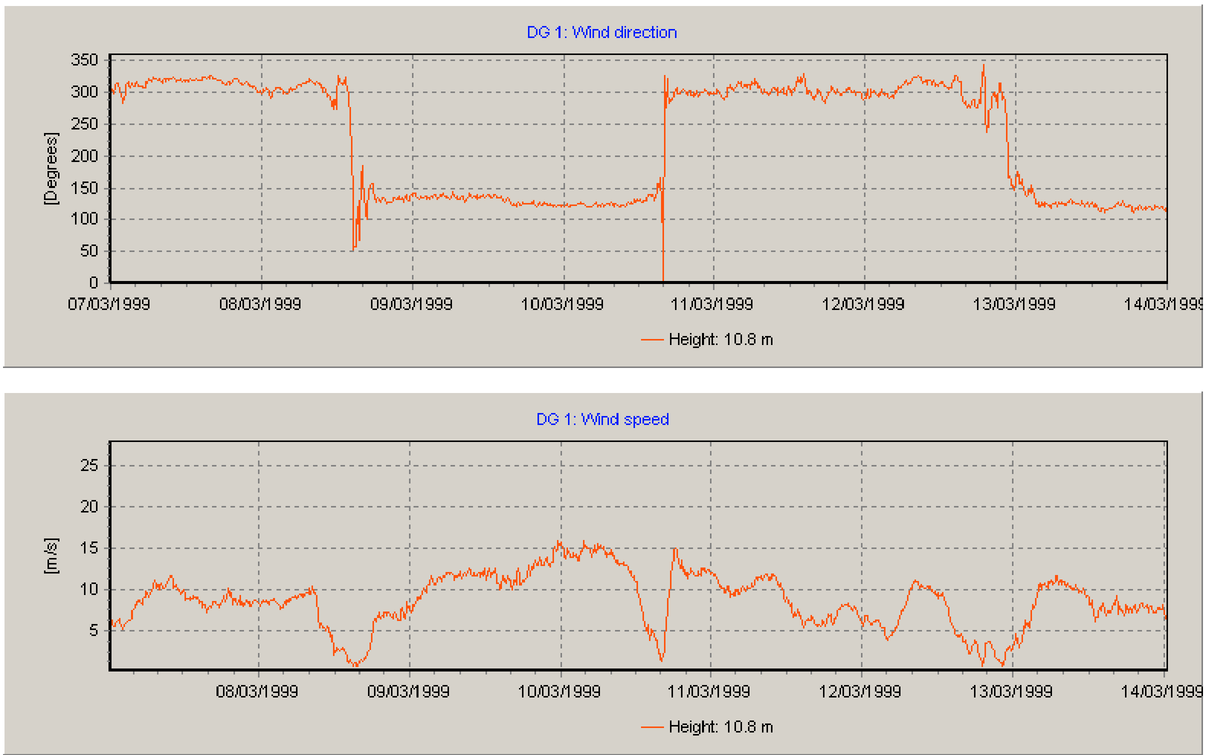

Figure 11: Sudden wind direction changes

4.3 Daily and Seasonal Variations

The wind speed data measured on-site (red line) shows a clear daily cycle with highest wind speeds in the morning but constant wind speed in the late afternoon and during the night (Figure 12).

The seasonal analysis shows significantly lower wind speed during the summer than during winter.

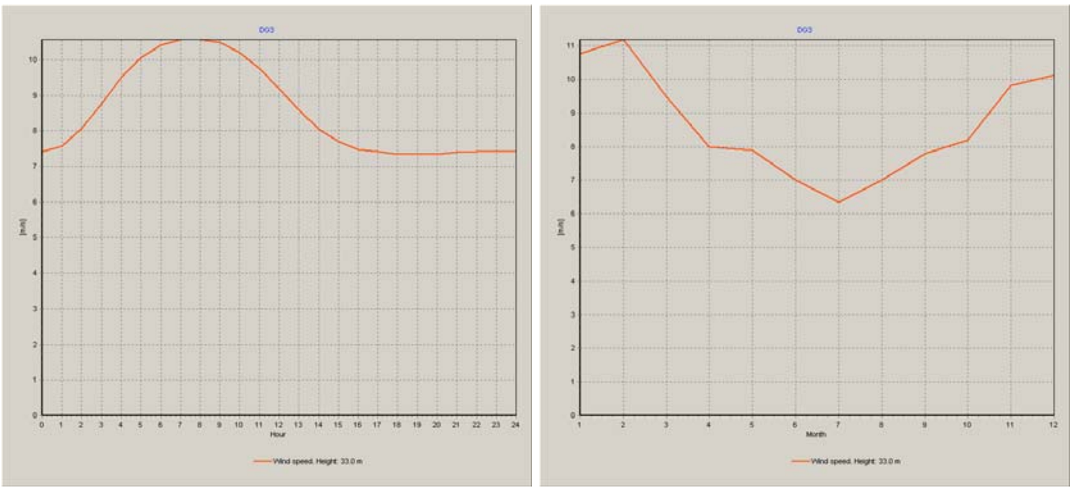

Figure 12: DG 2: Daily and seasonal variations 26.6m

5 Long-term Correction

In the assessment of the wind regime at a potential wind farm site it is generally necessary to correlate data recorded on the site with data recorded from a nearby long-term reference meteorological station. Wind data at a site are often only recorded for a short period and such correlation is required to ensure that the estimates of the wind speeds at the site are representative of the long-term. When selecting an appropriate meteorological station for this purpose it is important that it should have good exposure and that data are consistent over the measurement period being considered.

The meteorological station located at Zhalanashkol has been identified by the client as a potential reference station. This station is situated 20 km NW of the site at the north-westerly shore of lake Zhalanashkol (45°35'' N 82°07''E). The instrumentation consists of a weathercock mounted 10m above ground /4/.

Wind data have been supplied to Wind Solutions for the period from 1990 to 2000. The data consists of daily mean wind speeds which are derived by manual measurements every 3 hours for a period of 2 minutes, 8 times per day. Furthermore a monthly frequency distribution table of the wind direction for 16 sectors has been provided. Unfortunately a time series containing wind speed and direction simultaneously has not been provided. Hence no wind direction sector-wise long-term correction of the data is possible. Unfortunately the months January and May 1995, June and July 1996 and January 1999 are missing.

Please note that the provided long-term data varies in its extent from the data provided for earlier reports /7/.

5.1 Data Analysis

In a first step the consistency of the data set from Zhalanashkol has been checked. The following graph shows the monthly mean wind speeds from 1990 to 2000 from the meteorological station Zhalanashkol. Apparently the data is free of any trend.

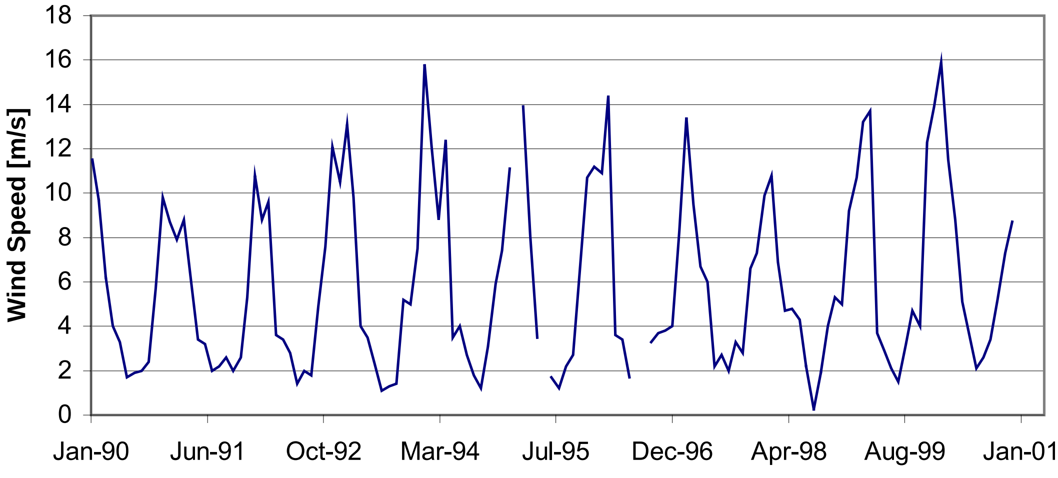

Figure 13: Time Series Zhalanashkol

However especially in Winter 1999/2000 wind speeds frequently exceed even 30m/s. Doubts are expressed about the validity because at these wind speeds it is not possible to stand upright anymore and buildings are damaged. It was therefore decided to exclude this period from the analysis.

In the next step the correlations between all on-site measurements and Zhalanashkol were checked. For the missing months in the data set of Zhalanashkol it has been assumed that the long-term average of the relevant months can be used.

Some values from the on-site data sets were identified as faulty and excluded from the further analysis. All data set are well correlated with each other (Table 6).

	DG 1 10	DG 2 26	DG 2 10	DG 3 33	DG 3 10	DG 4 33	DG 4 10	Zhalanashkol
DG 1 10	-	98.8%	98.8%	98.1%	98.4%	98.6%	89.9%	91.2%
DG 2 26		-	99.6%	87.5%	87.6%	90.9%	86.7%	87.3%
DG 2 10			-	89.6%	90.1%	93.5%	88.7%	88.2%
DG 3 33				-	99.5%	96.5%	91.1%	93.0%
DG 3 10					-	96.9%	91.6%	93.8%
DG 4 33						-	94.5%	95.9%
DG 4 10							-	90.9%

Table 6: Correlation R^2

A very high correlation between the on-site measurements but also with the long-term data set from Zhalanashkol could be shown. It is hence proven that Zhalanashkol is a suitable station to perform the long-term correction of the data set. However care should be taken since the accuracy of the data is given with 1-2 m/s /2/.

5.2 Data Correction

The data gap in January 1999 of Zhalanashkol has been filled with synthesised data on the basis of the mathematical relationship between the reference station and DG 4 since the correlation is highest.

Since it was concluded that the measurements performed at Zhalanashkol during the winter 1999/2000 are not trustworthy, the long-term correction has been performed on the basis of the data from May 1990 to April 1999, hence 9 years.

Because any seasonal bias must be avoided only an integer number of years of data can be used. Hence the analysis focuses on the period form May 1998 to April 1999. The advantage is that the data for that period is complete and available for all four masts.

The average wind speed at Zhalanashkol during the period from May 1998 to April 1999 is 5.91 m/s while the 9-year average is 5.67 m/s. Hence the period of on-site measurements is 4% windier than the long-term average.

The following tables summarise the long-term corrected wind speeds and Weibull parameters. More detailed results can be found in the Appendix.

	Height [m]	A-parameter	Mean Wind Speed [m/s]	k-parameter
DG 1	10.8	8.2	7.3	1.99
DG 2	26.6	9.3	8.2	1.98
	10.8	8.2	7.3	1.88
DG 3	33	9.3	8.2	2.10
	10.7	7.8	6.9	2.01
DG 4	33.1	9.5	8.4	1.92
	10.6	8.1	7.2	1.83

Table 7: Long-term corrected wind speeds and Weibull parameters

6 Flow Model

To calculate the variation of mean wind speed over the site, the computer wind flow model WAsP has been used. Details of the model and its validation are given by Troen and Petersen /5/. The inputs to the model are wind data, a digitised map of the topography and surface roughness length of the terrain for the site and surrounding area as well as a description of surrounding obstacles. A digitised map of the topography of a minimum of 15km around the site has been used. Although this domain size is much larger than the area of the site itself, such an area is necessary since the flow at any point is dictated by the terrain several kilometres upwind.

The wind flow is also affected by the roughness of the ground. Therefore the surface roughness length of the site and surrounding area has been estimated 15km around the site.

The wind flow calculations have been carried out for 30 degree steps in wind direction corresponding to the measured wind rose and results are produced as speed-up factors relative to the mast location for a grid encompassing the site area. All directions are then summed to obtain the mean wind speed at the required location.

The model assumptions were checked by cross-predicting the wind speeds at the different mast positions. The deviations between prediction and real measurements is within 0.1m/s, which is acceptable considering the low quality of the provided topographic maps and the limited information about surface roughness and surrounding obstacles.

Since the proposed layouts are close to DG 1 and DG2, DG 3 and 4 have not been used for the calculation of the energy yield. The energy yield calculation focus on the wind resource measured at DG 2 because of the significantly higher measurement height than DG1.

7 Wind Load Parameter

7.1 Air Density

The temperatures has been measured at different heights above ground on site. Temperatures from –26° to up to 40° have been measured (10-minute mean, 4.7m above ground).

The average annual mean temperature at 4.7m above ground level is 8.8°C. Hence the air density is 1.167kg/m³. Please note that no information has been provided about long-term temperatures on site.

Please note that the large variation of the temperature and the related change of air density makes the site less suitable for stall-regulated wind turbines as their pitch setting is adjusted to one specific air density. If the air density varies greatly a stall-regulated wind turbine would operate for significant periods of time outside the optimum parameters.

7.2 Turbulence

The ambient turbulence intensity can be determined on the basis of the on-site measurements. The followings graphs show the turbulence intensity measured at DG 2 versus wind speed (left) and the resulting turbulence intensity rose (right). Please note that wind speeds smaller than 4m/s have been suppressed in the following graphs.

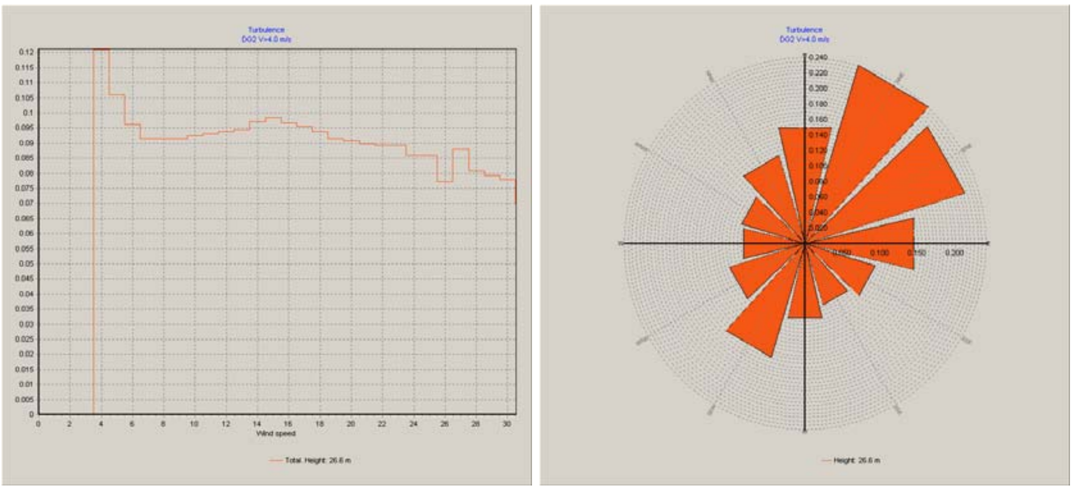

Figure 14: Turbulence intensity versus wind speed (left) and direction (right) at 26.6m height

Figure 14 indicates a turbulence intensity of less than 10% at 15 m/s averaged over all directions. The turbulence intensity rose shows the highest values from NNE. Since this is the direction of the lowest wind speed and the direction of the mast the measured values tie very well up with the theory.

The turbulence intensity will decrease with height above ground. In an conservative approach the turbulence intensity at hub height is estimated as 10% at 15 m/s averaged over all directions.

7.3 Mean Wind Speed at Hub Height

Wind flow modelling was carried out to determine the hub height wind speed variations over the site relative to the anemometry mast. The variations in wind speed has been predicted using WAsP computational flow model.

The wind flow model has been initiated from the measured wind speed and direction frequency distribution derived from the wind regime measured at DG 2 at 26.6m height.

Following tables display the frequency distribution at the location of DG 2 at an assumed hub height of 55m respectively 65m.

Sector	A-parameter [m/s]	Wind speed [m/s]	k-parameter	Frequency [%]
0 N	10.48	9.28	2.209	1.9
1 NNE	3.10	3.44	0.822	0.5
2 ENE	4.25	3.97	1.232	0.3
3 E	13.60	12.05	2.174	3.4
4 ESE	14.88	13.21	2.537	20.1
5 SSE	10.49	9.29	2.178	16.9
6 S	7.55	6.74	1.705	3.9
7 SSW	6.28	5.57	2.432	2.1
8 WSW	7.63	6.87	3.572	7.8
9 W	7.39	6.57	2.721	9.8
10 WNW	9.29	8.33	3.295	21.1
11 NNW	11.04	9.89	3.232	12.3
All	10.57	9.37	2.057	100.0

Table 8: Frequency Distribution at DG2 at 55m

Sector	A-parameter [m/s]	Wind speed [m/s]	k-parameter	Frequency [%]
0 N	10.82	9.58	2.252	1.9
1 NNE	3.22	3.56	0.830	0.5
2 ENE	4.44	4.14	1.248	0.3
3 E	13.99	12.39	2.193	3.5
4 ESE	15.25	13.54	2.561	20.1
5 SSE	10.80	9.56	2.221	16.9
6 S	7.84	6.99	1.736	3.9
7 SSW	6.58	5.84	2.475	2.1
8 WSW	8.01	7.22	3.643	7.8
9 W	7.73	6.88	2.771	9.8
10 WNW	9.67	8.69	3.365	21.0
11 NNW	11.41	10.23	3.295	12.2
All	10.94	9.69	2.104	100.0

Table 9: Frequency Distribution at DG2 at 65m

7.4 Extreme Wind Speed

The prediction of the 50-year extreme wind speed following the Gumbel distribution requires a representative set of data free of seasonal bias. Hence only data periods covering an integer number of years should be used. The following analysis has been performed for two complete years of DG 2 as this data set has been measured closest to the future wind turbines.

The 50-year maximum 10 minute mean wind speed has been estimated following the standard procedure by fitting a Gumbel type distribution to ranked periodic maximum values.

For every month of the two year long data sets the highest 10 minute mean wind speeds have been found. These wind speeds are ranked according to their value. A probability P is assigned and calculated as P=m/(N+1), where m is the rank and N the size of the sample. The slope of the linear regression applied to those points is used to calculate the 50-year wind speed.

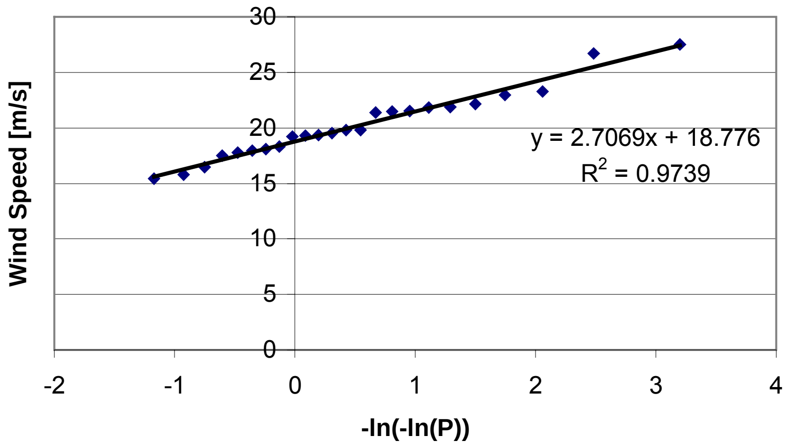

Figure 15: Gumbel plot DG 2 26.6m height

WAsP can be used to determine the speed-up factors from the position of the mast to hub height. The resulting speed-up is 1.06 to a hub height of 55m and 1.09 for a hub height of 65m for ESE.

The 50-year maximum 3-sec gust $V_{50,gust}$ at hub height is estimated using the relationship $V_{50,gust}=V_{50,10\text{-minute}}$ (1+ 3TI). The turbulence intensity TI at the 50 year maximum 10 minute mean wind speed is estimated to 10%. Hence the extreme wind speed results in:

Hub Height	10-Minute 50y max at hub height [m/s]	50y max gust at hub height [m/s]
55m	38.5	50.0
65m	39.4	51.2

Table 10: Extreme Wind Speeds at Hub Height

8 Layout

8.1 General

The future wind turbines are located close to the existing 10kV line.

Furthermore the distance to the road which runs parallel to the 10kV line was kept small to avoid costs for infrastructure.

Since the wind resource is bi-directional a layout has been chosen with minimum distances of the equivalent of three rotor diameter. It was not necessary to plan more than one row.

The wind turbines are located west of the masts DG1 and DG2. A distance of minimum 100m was kept to the existing overhead lines.

8.2 WTs with less than 55m rotor diameter

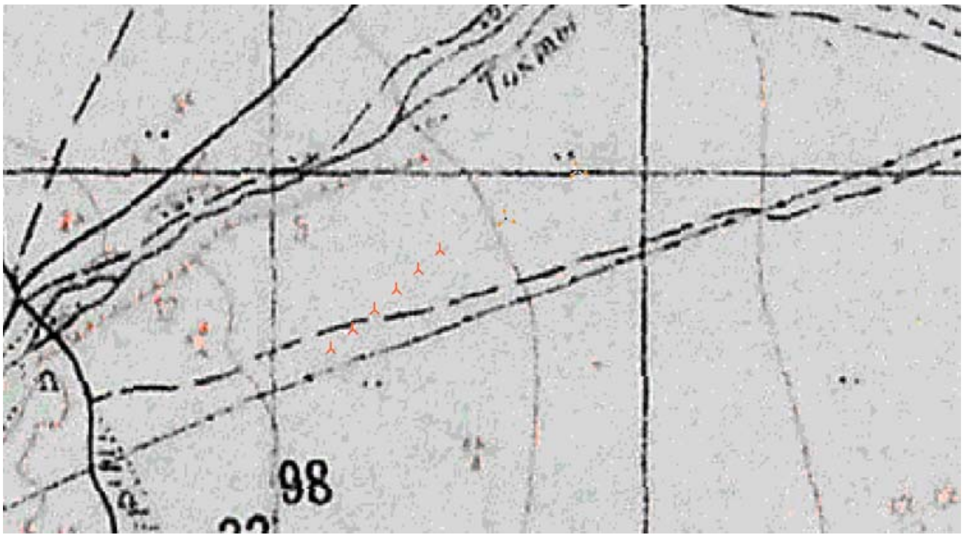

Figure 16: Layout WTs with less than 55m rotor diameter

The following table gives the co-ordinates in Gauss Krassowskij 6° zone 14.

	GK (Krass. 6 Deg) Zone: 14		
	East	North	Z [m]
1 New	14,598,296	5,033,082	549
2 New	14,598,414	5,033,184	545
3 New	14,598,533	5,033,286	541
4 New	14,598,651	5,033,388	536
5 New	14,598,769	5,033,490	532
6 New	14,598,888	5,033,593	528

Table 11: Co-ordinates WTs with less than 55m rotor diameter

8.3 WTs with more than 60m rotor diameter

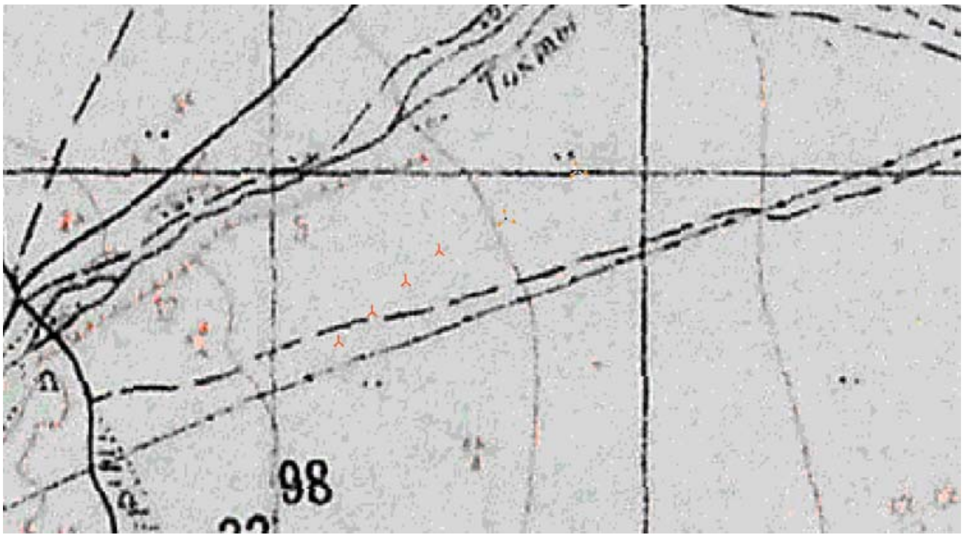

Figure 17: Layout WTs with more than 60m rotor diameter

The following table gives the co-ordinates in Gauss Krassowskij 6° zone 14. In case of the layout for the 2MW wind turbine only positions 1 to 3 are valid.

	GK (Krass. 6 Deg) Zone: 14		
	East	North	Z [m]
1 New	14,598,336	5,033,117	547
2 New	14,598,518	5,033,274	541
3 New	14,598,700	5,033,431	535
4 New	14,598,882	5,033,589	528

Table 12: Layout WTs with more than 60m rotor diameter

9 Energy Yield

9.1 Ideell Yield

Wind flow modelling was carried out to determine the hub height wind speed variations over the site relative to the anemometry mast. The variations in wind speed has been predicted using WAsP computational flow model.

The wind flow model has been initiated from the measured wind speed and direction frequency distribution derived from the wind regime measured at DG 2 at 26.6m height.

Following tables display the resulting energy yield. Please note that low hub heights have been chosen due to the very good wind resource.

Type	Capacity [MW]	Nr	Hub Height [m]	Total Capacity [MW]	Energy Yield [GWh/y] incl. park efficiency	Park Efficiency [%]	Equivalent Full Load Hours [h]
G52	0.85	6	55	5.1	21.1	98.3	4144
V52	0.85	6	55	5.1	20.8	98.2	4077

Table 13: Energy Estimate for WTs with less than 55m rotor diameter

Type	Capacity [MW]	Nr	Hub Height [m]	Total Capacity [MW]	Energy Yield [GWh/y] incl. park efficiency	Park Efficiency [%]	Equivalent Full Load Hours [h]
Siemens	1.3	4	60.0	5.2	21.4	98.7	4116
GE SE	1.5	4	64.7	6.0	26.6	98.7	4433
MM70	2.0	3	65.0	6.0	23.5	99.0	3917

Table 14: Energy Estimate for WTs with more than 60m rotor diameter

9.2 Losses

Following sources of losses have been considered.

The electrical transmission efficiency inside the wind farm has been assumed to be 98%. **No** allowance for utility downtime has been included in these results

A figure of 97% has been assumed for availability based on data from modern operational wind farms. The availability of the wind farm will be covered by a manufacturer's warranty for the first years of operation of the wind farm. Wind Solution has not reviewed the warranty contract for the wind farm so the above assumed level of availability should be considered in conjunction with the terms of the warranty agreement.

The turbine production may be affected by the build up of insects, dirt or ice on the blades. This build up will change the characteristics of the blade and therefore effect the performance of the blades and the turbine output. A figure of 97.0 % has been assumed to be appropriate.

Losses due to high wind hysteresis have been estimated by assessing the possible effect of high wind shut down and restart of the turbine. The magnitude of this lost production has been estimated by Wind Solution by repeating the analysis using a power curve with the output set to zero for the highest three wind speed bins.

Turbine	G52	V52	Siemens 1.3	GE 1.5 SE	MM70
Hub Height [m]	55	55	60	64.7	65
Capacity WT [MW]	0.85	0.85	1.3	1.5	2
Total capacity [MW]	5.1	5.1	5.2	6.0	6.0
Calculated Output [GWh/y]	21.1	20.8	21.4	26.6	23.5
Electrical efficiency [%]	98%				
Availability [%]	97%				
Icing and blade degradation [%]	97%				
High wind speed hysteresis [%]	98.3%	98.3%	98.1%	98.1%	98.5%
Net output [GWh/y]	19.2	18.8	19.4	24.1	21.3

Table 15: Losses in the Wind Farm

9.3 Uncertainty

Following sources of uncertainty have been identified:

9.3.1 Wind Speed

The uncertainty of the wind speed measurements on site relates to the calibration error, mounting and 2nd order effects like degradation, icing, ageing of bearings, turbulence etc.

- The uncertainty associated with the calibration of the anemometers is estimated at 1.5%.
- The uncertainty associated with the mounting of the anemometers is estimated at 0.5%.
- The uncertainty associated with second order effects such as degradation, icing, ageing of bearings, turbulence. A total uncertainty of 1% is assumed for these effects.

The uncertainties above are added as independent errors on a root-sum-square basis to give the total uncertainty in the site wind speed measurement as 1.9%.

The uncertainty of the wind speed measurements at the reference station relates to the calibration error, mounting and 2nd order effects like degradation, icing, ageing of bearings, turbulence etc. Additionally inter-annual variations and the prediction error in the long-term correlation has to be taken into account.

- The uncertainty of the wind speed measurements at the long-term met site, taking into account the lack of information regarding the installation at the long-term station, and the precise data format, is estimated at 4%.
- There is an uncertainty associated with the assumption made here that the historical period at the meteorological site is representative of the climate over longer periods. A study of the Zhalanashkol data indicates a variability of 8.3 % in the annual mean wind speed. Taking into account prediction and historic periods of 10 years each, this gives an uncertainty due to inter-annual variation of 3.7%.
- The uncertainty due to the prediction methodology is estimated at 0.01%

Combined uncertainty in the long-term mean wind speed on site is estimated at 5.03%.

The total uncertainty in the wind speed including the on-site and reference station sums up to 5.77%.

9.3.2 Flow Modelling

1. Topographic modelling uncertainties

   For this development an uncertainty in topographic modelling of 5% is assumed because the mast height is less than the turbine hub height /6/.

2. Wake modelling uncertainties

   An uncertainty due to the inaccuracy of the model determining the park efficiency is estimated to half the park losses due to shadowing of the wind farm.

The uncertainties above are added as independent errors on a root-sum-square basis to give the total uncertainty in the flow modelling.

9.3.3 Power Curve Uncertainties

No documentation of the uncertainty related to the power curves has been made available. Hence the uncertainty can only be estimated. An uncertainty of 7% of the AEP is assumed.

9.3.4 Summary

The identified uncertainties are summarised in following tables.

For the pilot WT the uncertainty related to the park model is not relevant.

	Wind Speed Uncertainty	Production Uncertainty G52	Production Uncertainty V52	Production Uncertainty Siemens 1.3	Production Uncertainty GE 1.5SE	Production Uncertainty MM70
On-site Measurer	1.87%					
LT correction	5.77%					
Sub Total	**5.77%**	**7.4%**	**7.4%**	**7.4%**	**7.1%**	**8.1%**
Flow Modell		5.1%	5.1%	5.0%	5.0%	5.0%
Power Curve		7.0%	7.0%	7.0%	7.0%	7.0%
Sub Total		**8.6%**	**8.6%**	**8.6%**	**8.6%**	**8.6%**
Overall Uncertainty		**11.4%**	**11.4%**	**11.4%**	**11.2%**	**11.8%**

Table 16: Estimate of Uncertainties of the Park

The uncertainties represent the standard deviation of what is assumed to be a Gaussian process: There is therefore a 50% chance that, even when taken over very long periods, the mean energy production will be less than the value given in the Table 15. The error associated with the prediction of energy capture has been calculated and the confidence limits for the prediction are given in the tables below :

Probability of Exceedance	AEP G52 [MWh/y]	AEP V52 [MWh/y]	AEP Siemens 1.3 [MWh/y]	AEPGE 1.5 SE [MWh/y]	AEP MM70 [MWh/y]
95%	15577	15324	15748	20166	17398
90%	16368	16101	16547	21172	18326
85%	16902	16626	17086	21850	18952
80%	17326	17043	17514	22389	19450
75%	17690	17401	17881	22852	19877
70%	18016	17722	18211	23267	20260
65%	18319	18020	18517	23652	20616
60%	18607	18302	18807	24017	20953
55%	18885	18576	19088	24370	21279
50%	**19158**	**18845**	**19364**	**24718**	**21600**
45%	19432	19114	19640	25066	21921
40%	19710	19387	19921	25419	22247
35%	19997	19669	20211	25784	22584
30%	20300	19967	20516	26169	22940
25%	20627	20288	20846	26584	23323
20%	20990	20646	21214	27047	23750
15%	21414	21063	21642	27586	24248
10%	21948	21588	22181	28264	24874
5%	22739	22365	22979	29270	25802

Table 17: Probability of Exceedance of the AEP

10 Comments and Recommendations

A high impact on the certainty of the uncertainty of the energy yield is introduced due to the relatively low measurement heights (Chapter 9.3.1). The uncertainty could be reduced by employing higher measurement heights.

Please note that due to the narrowness of Djungar Gate, the geographical representativeness of the measured wind climate has a limited extent. The applicability of the wind data to estimate the wind climate of the surrounding regions is strongly limited by the complexity of the terrain and is estimated as five kilometres up and down the valley from the sites.

Please note that the rapid wind direction changes (Figure 11) put a significant strain on the mechanical structure of the wind turbines. The control system has to be adjusted accordingly.

Considering the strong changes in air density during the course of the year stall-regulated wind turbines might not be suitable for the site.

11 Reference

/1/ Wind speed profiles over terrain with roughness change, Engineering Sciences Data, Item no. 84011, April 1993

/2/ E-mail from G. Doroshin, 17.8.05 and 27.8.05

/3/ IEA: Recommended Practices for Wind Turbine Testing, Part 11. Wind Speed Measurement and Use of Cup Anemometry, 1999

/4/ E-mail from G. Doroshin, 19.8.05

/5/ I. Troen and E. L. Petersen, “European Wind Atlas”, Risø National Laboratory, Denmark, 1989

/6/ A. Albers: Uncertainty Analysis of Energy Yield Predictions as Basis for Risk Evaluation of Wind Farm Projects, Proceedings DEWEK 2002, Wilhelmshaven, Germany, 2002

/7/ E.L. Petersen, O.F. Hansen, G. Jensen: Djungar Gate and Chilik Corridor – Kazakhstan, Risø National Laboratory, Denmark, 1999

Appendix